 CMES, vol.44, no.2, pp.157-175, 2009

Numerical Modelling of Electromagnetic Waves by Explicit Multi-Level Time-Step FEM-BEM Coupling Procedures

Delfim Soares Jr.[1]

Abstract: The numerical modelling of electromagnetic waves by finite element – boundary element coupling procedures is discussed here, taking into account time-domain approaches. In this study, the global model is divided into different sub-domains and each sub-domain is analysed independently and explicitly at each time-step of the analysis: the interaction between the different sub-domains of the global model is accomplished by interface procedures. A multi-level time-step algorithm is considered in order to improve the flexibility, accuracy and stability (especially when conditionally stable time-marching procedures are employed) of the coupled analysis. At the end of the paper, numerical examples are presented, illustrating the potentialities and robustness of the proposed methodologies.

Keywords: Finite Elements; Boundary Elements; Time-Domain Analysis; Multi-Level Time-Steps; Electromagnetic Waves; Green-Newmark Method.

1 Introduction

Along the last decades, the Finite Element Method (FEM) and the Boundary Element Method (BEM) have been successfully applied to analyse a great sort of physical problems, as for instance, the numerical simulation of complex electromagnetic fields. For certain categories of problems, however, neither the FEM nor the BEM is best suited (e.g., the propagation of electromagnetic waves through infinite inhomogeneous media) and it is natural to attempt to couple these two methods in an effort to create a numerical procedure that combines all their advantages and reduces their disadvantages. Up to now, although a considerable amount of publications is available considering FEM-BEM coupled analyses, few publications concentrate on the topic when time-domain electromagnetic modelling is focused.

[1] Faculty of Engineering, Federal University of Juiz de Fora, Cidade Universitária, CEP 36036-330, Juiz de Fora, MG, Brazil. Tel: +55 32 2102-3468; E-mail: delfim.soares@ufjf.edu.br

According to Jiao *et al.* (2001), the first works on the theme seem to date from the beginning of the decade. Jiao *et al.* (2001) presented a time-domain finite element – boundary integral method to analyse electromagnetic scattering from two-dimensional inhomogeneous objects. Later on, alternative approaches have been proposed and three-dimensional analyses have been considered (Jiao *et al.*, 2002; McCowen *et al.*, 2003; Qiu *et al.*, 2007; Yılmaz *et al.*, 2007; Soares, 2008a). Taking into account transformed-domain analyses (especially frequency-domain analyses), FEM-BEM coupling techniques are well established, and several works are currently available considering electromagnetic modelling (Stupfel, 2001; Liu and Jin, 2001, 2002; Tzoulis and Eibert, 2005; Botha and Jin, 2005; Eibert, 2007). For other related publications, the reader is referred to Young and Ruan (2005), Ha *et al.* (2006), Takei *et al.* (2008), Liu (2008) etc..

In all time-domain FEM-BEM coupling algorithms published so far to analyse the propagation of electromagnetic waves, an equal-value time-step is adopted to discretize all coupled sub-domains, indifferently if they are modelled by the FEM or by the BEM. This may lead to some numerical difficulties, once quite different optimal temporal discretizations are usually required by these two numerical techniques. For small time-steps, the time-domain BEM may become unstable, whereas, for large time-steps, excessive numerical damping may occur. The FEM, on the other hand, usually requires small time-steps to preserve accuracy and/or to ensure stability.

In the present work, two-dimensional models are focused and a multi-level time-step algorithm is presented in order to analyse sub-domains spatially discretized by the FEM, and temporally discretized by the Central Difference Method or by the Green-Newmark Method, coupled with sub-domains spatially and temporally discretized by the time-domain BEM. The Green-Newmark Method is a time-marching technique, developed by the author (Soares and Mansur, 2005a; Soares, 2007), which can be very effective when dealing with coupled models, as it has been previously illustrated considering some computational mechanic applications (Soares and Mansur, 2005b; Soares *et al.*, 2007; Soares, 2008b). As is well known, the Central Difference Method is a conditionally stable technique (i.e., a critical time-step must be respected in order to ensure the stability of the method); thus, a multi-level time-step approach is of great importance regarding FEM-BEM coupling procedures based on this time-marching technique.

Taking into account the above-described FEM time-marching procedures, FEM sub-domains can be analysed independently at each time step, considering only BEM previous time-steps results. This allows the time-domain FEM-BEM coupled system of equations to be properly uncoupled at the current time-step of the analysis and, as a consequence, the presently proposed technique becomes very attractive: FEM and BEM sub-domains (optimally spatially and temporally discretized) can be analysed separately, leading to smaller and better-conditioned systems of equations, which can be independently solved by most suitable numerical procedures.

The present work is organized as follows: first, the governing equations are presented and their discretization by finite and boundary element techniques is briefly described; next, the proposed FEM-BEM coupling algorithms are discussed, taking into account the multi-level time-step methodology. At the end of the paper, numerical applications are considered, illustrating the accuracy and robustness of the proposed formulations.

2 Governing equations

Maxwell's equations in differential form can be written as:

$$e_{ijk}E_{k,j} = -\dot{B}_i \tag{1a}$$

$$e_{ijk}H_{k,j} = \dot{D}_i + J_i \tag{1b}$$

$$D_{i,i} = \rho \tag{1c}$$

$$B_{i,i} = 0 \tag{1d}$$

where indicial notation for Cartesian axes is considered and e_{ijk} stands for the permutation symbol (also known as alternator tensor). Inferior commas and overdots indicate partial space and time derivatives, respectively (i.e., $V_{i,j} = \partial V_i/\partial x_j$ and $\dot{V}_i = \partial V_i/\partial t$, where $V_i(X,t)$ stands for a generic vector field representation and X and t denote its spatial and temporal arguments, respectively).

In equations (1), E_i and H_i are the electric and magnetic field intensity components, respectively; D_i and B_i represent the electric and magnetic flux density, respectively; and J_i and ρ stand for the electric current and electric charge density, respectively. The constitutive relations between the field quantities are specified as:

$$D_i = \varepsilon E_i \tag{2a}$$

$$B_i = \mu H_i \tag{2b}$$

$$J_i = \sigma E_i \tag{2c}$$

where the parameters ε, μ and σ denote, respectively, the permittivity, permeability and conductivity of the medium.

Combining equations (1) and (2), vectorial wave equations describing the electric and the magnetic field can be obtained, as is indicated below:

$$e_{mni}(\mu^{-1}e_{ijk}E_{k,j})_{,n} + \varepsilon \ddot{E}_m = -\dot{J}_m \tag{3a}$$

$$e_{mni}(\varepsilon^{-1}e_{ijk}H_{k,j})_{,n} + \mu\ddot{H}_m = e_{mni}(\varepsilon^{-1}J_i)_{,n} \tag{3b}$$

where the wave propagation velocity of the medium is specified as $c = (\varepsilon\mu)^{-1/2}$.

Taking into account two-dimensional applications, equations (3) can be simplified and written in a unique general form:

$$(\kappa^{-1}\phi_{,i})_{,i} - \nu\ddot{\phi} = \gamma \tag{4}$$

where ϕ is a generic representation for an electric (E_k) or magnetic (H_k) field intensity component (e.g., $i = 1,2$ and $k = 3$) and γ stands for a generic source term. κ and ν represent μ or ε, according to the case of analysis.

Once the governing differential equation is established, temporal and spatial boundary conditions must be defined. The spatial boundary conditions for the model in focus are:

$$\phi = \bar{\phi} \tag{5a}$$

$$\theta = \phi_{,i}n_i = \bar{\theta} \tag{5b}$$

where equation (5a) stands for essential (or Dirichlet) boundary conditions and equation (5b) stands for natural (or Neumann) boundary conditions (n_i represents an outward unit vector normal to the boundary). In equations (5), overbars indicate prescribed values.

At the interface between two media, field continuity conditions are defined as:

$$(\phi)_+ = (\phi)_- \tag{6a}$$

$$(\kappa^{-1}\theta)_+ = -(\kappa^{-1}\theta)_- \tag{6b}$$

which are of great importance in a FEM-BEM coupling context.

In the sections that follow, the numerical discretization of the above-presented governing equations is briefly discussed, taking into account finite element and boundary element techniques. In the sequence, the FEM-BEM coupling algorithms are presented.

3 Finite element modelling

In a finite element approach, the incognita field is spatially interpolated within the element, as indicated below:

$$\phi(X,t) = N_\alpha(X)\phi_\alpha(t) \tag{7}$$

where N represents element spatial interpolation functions and greek subscripts stand for an element internal numeration (element nodes or edges).

Taking into account electromagnetic wave propagation phenomena, the time-domain system of equations that arises, once finite element spatial discretization is considered (equation (7)), is given by:

$$\mathbf{M}\ddot{\mathbf{\Phi}}^n + \mathbf{K}\mathbf{\Phi}^n = \mathbf{F}^n \tag{8}$$

where $\mathbf{\Phi}$ is a generic vector describing electric or magnetic field components and $\mathbf{F}$ is a vector of generalized applied sources. The superscript n stands for the current time of analysis. The matrix and vector entries involved in equation (8) are defined, at element level, as:

$$M_{\alpha\beta} = \int_{\Omega_e} \nu N_\alpha N_\beta \, d\Omega \tag{9a}$$

$$K_{\alpha\beta} = \int_{\Omega_e} \kappa^{-1} (N_{,i})_\alpha (N_{,i})_\beta \, d\Omega \tag{9b}$$

$$F_\alpha = \int_{\Gamma_e} N_\alpha \, \kappa^{-1} \bar{\theta} \, d\Gamma - \int_{\Omega_e} N_\alpha \, \gamma d\Omega \tag{9c}$$

where Γ_e and Ω_e stand for the boundary and the domain of the element, respectively.

In order to discretize equation (8) in the time domain, two methodologies are considered here, namely: the Central Difference Method (which is a commonly used time-marching technique) and the Green-Newmark Method (Soares and Mansur, 2005a; Soares, 2007). These methodologies are briefly discussed in the sub-sections that follow.

3.1 Central Difference Method

In the Central Difference Method, the following finite difference relation is considered:

$$\ddot{\mathbf{\Phi}}^n = (1/\Delta t^2)\,(\mathbf{\Phi}^{n+1} - 2\mathbf{\Phi}^n + \mathbf{\Phi}^{n-1}) \tag{10}$$

where Δt is the selected time-step. After introducing relation (10) into the system of equations (8), the following system of equations arises, which enables the computation of the transient FEM response at time t^n:

$$\mathbf{A}\mathbf{\Phi}^n = \mathbf{B}^{n-1} \tag{11}$$

In equation (11), $\mathbf{A}$ and $\mathbf{B}$ are the FEM effective matrix and vector, respectively, given by:

$$\mathbf{A} = (1/\Delta t^2)\mathbf{M} \tag{12a}$$

$$\mathbf{B}^{n-1} = \mathbf{F}^{n-1} - (\mathbf{K} - (2/\Delta t^2)\mathbf{M})\,\mathbf{\Phi}^{n-1} - (1/\Delta t^2)\mathbf{M}\mathbf{\Phi}^{n-2} \tag{12b}$$

3.2 Green-Newmark Method

The analytical expressions for $\mathbf{\Phi}^n$ and $\dot{\mathbf{\Phi}}^n$, which obey equation (8), are given by:

$$\mathbf{\Phi}^n = \dot{\mathbf{G}}^n \mathbf{M} \mathbf{\Phi}^0 + \mathbf{G}^n \mathbf{M} \dot{\mathbf{\Phi}}^0 + \mathbf{G}^n \cdot \mathbf{F}^n \tag{13a}$$

$$\dot{\mathbf{\Phi}}^n = \ddot{\mathbf{G}}^n \mathbf{M} \mathbf{\Phi}^0 + \dot{\mathbf{G}}^n \mathbf{M} \dot{\mathbf{\Phi}}^0 + \dot{\mathbf{G}}^n \cdot \mathbf{F}^n \tag{13b}$$

where $\mathbf{G}^n$ represents the Green's function matrix of the model, $\mathbf{\Phi}^0$ and $\dot{\mathbf{\Phi}}^0$ stand for initial conditions and the symbol $\cdot$ represents time convolution.

Assuming that a given time-step Δt is small enough, approximation (14) can replace the convolution integrals indicated in equation (13) (f_1 and f_2 are generic functions). It is important to notice that the approximations indicated in equation (14) are analogous to those employed in frequency domain analyses, where standard DFT/FFT algorithms are employed (Soares and Mansur, 2003), and they give the same results for most engineering problems as a two-point Newton-Cotes quadrature rule (Soares and Mansur, 2005a).

$$\int_0^{\Delta t} f_1(\Delta t - \tau)\, f_2(\tau)\, d\tau = f_1(0)\, f_2(\Delta t)\, \Delta t \tag{14}$$

Taking into account the approximations indicated by equation (14), recursive expressions can be obtained by considering equation (13) at time t^n and by supposing that the analysis begins at time t^{n-1}. The recurrence relations that arise are given by:

$$\mathbf{\Phi}^n = \dot{\bar{\mathbf{G}}} \mathbf{M} \mathbf{\Phi}^{n-1} + \bar{\mathbf{G}} \mathbf{M} \dot{\mathbf{\Phi}}^{n-1} + \mathbf{G}^0 \mathbf{F}^n \Delta t \tag{15a}$$

$$\dot{\mathbf{\Phi}}^n = \ddot{\bar{\mathbf{G}}} \mathbf{M} \mathbf{\Phi}^{n-1} + \dot{\bar{\mathbf{G}}} \mathbf{M} \dot{\mathbf{\Phi}}^{n-1} + \dot{\mathbf{G}}^0 \mathbf{F}^n \Delta t \tag{15b}$$

where $\bar{\mathbf{G}}$ is the Green's function matrix of the model at time-step Δt. $\bar{\mathbf{G}}$, as well as its time derivatives, can be evaluated properly by solving the system of equations (8) at time $t = \Delta t$, considering an excitation free model submitted to the following initial conditions: $\mathbf{G}^0 = \mathbf{0}$ and $\dot{\mathbf{G}}^0 = \mathbf{M}^{-1}$. In the present work, the Newmark method is applied to solve this initial condition problem. Initially, the Newmark method is employed to establish the expressions to compute $\bar{\mathbf{G}}$ and its time derivatives; subsequently, these expressions are introduced into the recurrence relations (15). The final recurrence relations that arise are then given by:

$$\mathbf{\Phi}^n = \mathbf{O}^n + (1 - \eta_2/\eta_1)\mathbf{\Phi}^{n-1} \tag{16a}$$

$$\dot{\mathbf{\Phi}}^n = (\eta_2/(\eta_1 \Delta t))\mathbf{O}^n - (1/(\eta_1 \Delta t))\,\mathbf{\Phi}^{n-1} + (1 - \eta_2/\eta_1)\dot{\mathbf{\Phi}}^{n-1} + \mathbf{M}^{-1}\mathbf{F}^n \Delta t \tag{16b}$$

In equations (16), η_1 and η_2 stand for the newmark parameters (the relation $\eta_2^2 = \eta_1$ is considered in order to achieve the final suitable expression (16b)) and $\mathbf{O}^n$ is computed by the solution of the following system of equations:

$$\mathbf{A}\mathbf{O}^n = \mathbf{B}^{n-1} \tag{17}$$

where

$$\mathbf{A} = \mathbf{K} + (1/(\eta_1 \Delta t^2))\mathbf{M} \tag{18a}$$

$$\mathbf{B}^{n-1} = \mathbf{M}((\eta_2/(\eta_1 \Delta t)^2)\mathbf{\Phi}^{n-1} + (1/(\eta_1 \Delta t))\dot{\mathbf{\Phi}}^{n-1}) \tag{18b}$$

Equations (16) enable the computation of the FEM responses at time t^n (lumped matrices can be considered when evaluating the last term in equation (16b), in order to avoid solving an extra system of equations). As it has been demonstrated (Soares and Mansur, 2005a), considering the trapezoidal rule (i.e., η_1 = 0.25 and η_2 = 0.50), the amplification matrix related to the solution algorithm (16) is second order accurate and unconditionally stable.

4 Boundary element modelling

In a boundary element approach, the incognita fields (mixed formulation) are temporally and spatially interpolated within the element, as indicated below:

$$\phi(X,t) = N_\alpha(X)\, M^m(t)\, \phi_\alpha^m \tag{19a}$$

$$\theta(X,t) = N_\alpha(X)\, M^m(t)\, \theta_\alpha^m \tag{19b}$$

where, once again, N represents element spatial interpolation functions and greek subscripts stand for an element internal numeration. M represents temporal interpolation functions (in the present work, linear and piecewise constant time interpolation functions are considered regarding the ϕ and θ incognita fields, respectively).

Taking into account electromagnetic wave propagation phenomena, the system of equations that arises, once time-domain boundary element spatial and temporal discretization is considered (equation (19)), is given by:

$$\mathbf{C}\mathbf{\Phi}^n = \mathbf{G}^{nm}\mathbf{\Theta}^m - \mathbf{H}^{nm}\mathbf{\Phi}^m + \mathbf{S}^n \tag{20}$$

where $m = 1, \ldots, n$; $\mathbf{C}$ is a geometric matrix and $\mathbf{G}$ and $\mathbf{H}$ are influence matrices. Once again, equation (20) stands for a general expression: $\mathbf{\Phi}$ is a generic vector describing electric or magnetic field components and $\mathbf{\Theta}$ is related to the spatial derivatives of these components. $\mathbf{S}$ is a vector accounting for generalized source terms.

The entries of the influence matrices involved in equation (20), as well as of the source vector, are given by:

$$G_{\alpha\beta}^{nm} = \int_{\Gamma} N_\beta \int_0^{t^n} \Phi_\alpha^n M^m \, d\tau \, d\Gamma \tag{21a}$$

$$H_{\alpha\beta}^{nm} = \int_{\Gamma} N_\beta \int_0^{t^n} \Theta_\alpha^n M^m \, d\tau \, d\Gamma \tag{21b}$$

$$S_\alpha^n = \int_{\Omega} \int_0^{t^n} \Phi_\alpha^n \gamma \, d\tau \, d\Omega \tag{21c}$$

where Φ and Θ are the fundamental solutions of the time-domain two-dimensional model. Φ is defined as follows ($\Theta = \Phi_{,i} n_i$):

$$\Phi_\alpha^n = \Phi(X, t^n; X_\alpha, \tau) = (c/2\pi)(c^2(t^n - \tau)^2 - r^2)^{-1/2} H\left[c(t^n - \tau) - r\right] \tag{22}$$

where $r = |X - X_\alpha|$ is the distance between the observation and the collocation point and H stands for the heaviside function.

After considering the boundary conditions of the problem, the following system of equations arises from expression (20), which enables the computation of the transient BEM response at time t^n:

$$\mathbf{A}\mathbf{X}^n = \mathbf{B}^n \tag{23}$$

In equation (23), **A** and **B** are the BEM effective matrix and vector, respectively, and the entries of **X** are the unknown variables (one should observe that vector **B** accounts for the current time-step boundary prescribed conditions, domain discretized terms and time convolution contributions).

5 FEM-BEM coupling

In this work, the global model is divided into different sub-domains and each sub-domain is analysed independently (as an uncoupled model), taking into account the numerical discretization techniques discussed in sections 3 and 4. The interactions between the different sub-domains of the global model are considered taking into account the field values at the common interfaces and the continuity equations (6). Two FEM-BEM coupling algorithms are discussed here, both considering explicit coupling techniques: in the first algorithm (algorithm 1), the Central Difference

Method and lumped matrices **M** are employed in the sub-domains discretized by the FEM. In the second algorithm (algorithm 2), the Green-Newmark Method is considered within the FEM sub-domains.

For both coupling algorithms, it is appropriate to consider different temporal discretizations within each sub-domain. This is the case since optimal FEM and BEM time-steps are usually quite different when homogeneous interfaces are analysed, especially taking into account the Central Difference Method, which is a conditionally stable time-marching methodology. As has been extensively reported in the literature, for small time-steps, the time-domain BEM may become unstable, whereas, for large time-steps, excessive numerical damping may occur. Thus, in order to ensure stability and/or accuracy, usually a much smaller FEM time-step is required when coupled FEM-BEM analysis of homogeneous interfaces is considered. In the next sub-section the adoption of different temporal discretizations within each FEM/BEM sub-domain is discussed. In the sequence, the coupling algorithms are described.

5.1 Multi-level time-step discretization

In order to consider different time-steps in each sub-domain, interpolation/extrapolation procedures along time are performed. In this work, the temporal interpolation/extrapolation procedures are based on the BEM time interpolation functions M (see equations (19)). Here, linear and piecewise constant time interpolation functions are considered regarding the ϕ and θ incognita fields, respectively, as depicted in Fig.1. Fig.1 describes the calculus of some time-interpolated/extrapolated variables that are important in the context of the FEM-BEM coupling algorithms presented in the next sub-section. In Fig.1(a), the extrapolation of the ϕ field at the current FEM time-instant t_F in order to compute its value at the current BEM time-instant t_B is illustrated (see equation (24a)). In Fig.1(b), the interpolation of the θ value at time t_B in order to compute its value at time t_F is depicted (see equation (24b)).

$$\phi^{t_B} = \phi^{t_F}(\Delta t_B/\Delta t_{FB}) + \phi^{t_B-\Delta t_B}(1-\Delta t_B/\Delta t_{FB}) \tag{24a}$$

$$\theta^{t_F} = \theta^{t_B} \tag{24b}$$

Using time interpolation/extrapolation procedures, optimal FEM and BEM modelling in each sub-domain may be achieved, which is very important regarding flexibility, efficiency, accuracy and stability.

5.2 Coupling algorithms

In the coupling algorithms considered here, natural boundary conditions are prescribed at the FEM common interfaces and essential boundary conditions are pre-

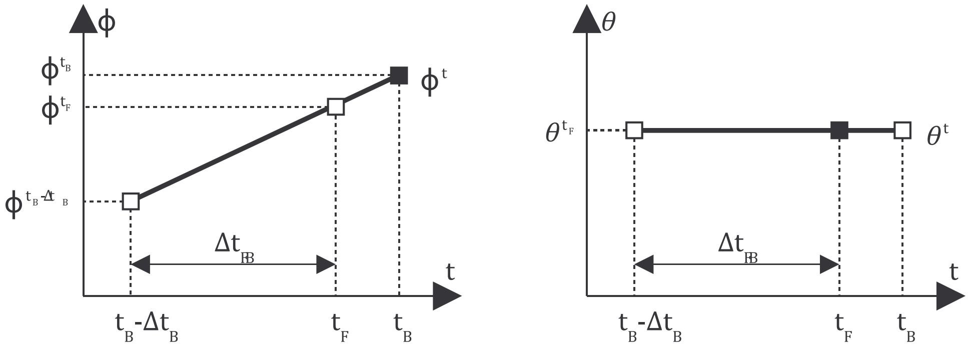

Figure 1: Time interpolation/extrapolation procedures: (a) extrapolation of ϕ^{t_F} in order to compute ϕ^{t_B}; (b) interpolation of θ^{t_B} in order to compute θ^{t_F}.

scribed at the BEM common interfaces. The ϕ fields related to the sub-domains modelled by the FEM are computed directly, since their evaluations only take into account BEM results corresponding to previous time-steps (see equation (11) or equation (16a)). Once the FEM ϕ fields are computed, they are employed as prescribed interface boundary conditions (essential boundary condition) for the sub-domains modelled by the BEM, and the BEM θ fields are computed. The BEM θ values are then employed to evaluate the FEM nodal forces (natural boundary condition) – as well as some other FEM variables, if necessary – and the next time-step computations are initiated, repeating the above-described procedures. The detailed coupling algorithms are presented below, taking into account different temporal discretizations within each BEM/FEM sub-domain.

Algorithm 1:

(1) FEM sub-domains analyses: evaluation of $\phi_F^{t_F}$ (equation (11));

(2) Interfaces compatibility: $\bar{\phi}_B^{t_F} = \phi_F^{t_F}$ (equation (6a));

(3) Time extrapolations: $\bar{\phi}_B^{t_B} = \bar{\phi}_B^{t_F}(\Delta t_B/\Delta t_{FB}) + \bar{\phi}_B^{t_B-\Delta t_B}(1-\Delta t_B/\Delta t_{FB})$(equation (24a));

(4) BEM sub-domains analyses: evaluation of $\theta_B^{t_B}$ (equation (23));

(5) Time interpolations: $\theta_B^{t_F} = \theta_B^{t_B}$ (equation (24b));

(6) Interfaces compatibility: $\bar{\theta}_F^{t_F} = -\,\theta_B^{t_F}(\kappa_B^{-1}/\kappa_F^{-1})$ (equation (6b)).

Algorithm 2:

(1) FEM sub-domains analyses: evaluation of $\phi_F^{t_F}$ (equation (16a));

(2-6) Same as in *Algorithm 1*;

(7) FEM sub-domains analyses: evaluation of $\dot{\phi}_F^{t_F}$ (equation (16b)).

As can be observed, by adopting lumped matrices **M** (see equation (12a)), algorithm 1 becomes very efficient: only BEM systems of equations must be dealt with, which are usually of reduced dimension. On the other hand, according to algorithm 2, two systems of equations must be dealt with independently at each time-step: one related to the BEM and another related to the FEM (see equation (17)). However, the FEM time-marching technique employed in algorithm 1 is conditionally stable, whereas, in algorithm 2, it is unconditionally stable, once appropriate Newmark parameters are considered (the Trapezoidal Rule, for instance). Thus, larger FEM time-steps may be considered in algorithm 2, which reduces the computational costs of the analysis.

6 Numerical Applications

In the next sub-sections, some numerical applications are presented, illustrating the potentialities of the proposed methodologies. In the first application, the electromagnetic field associated to an infinitely long wire, carrying a time-linear current, is analysed. In the second example, the electromagnetic wave propagation between two parallel lines of wires is discussed. The present work focuses on the analysis of homogeneous media (where standard time-domain FEM-BEM coupling procedures may become unstable), taking into account different time discretizations for each FEM/BEM sub-domain.

For all the applications that follow, within the FEM sub-domains, the trapezoidal rule ($\eta_1 = 0.25$ and $\eta_2 = 0.50$) is considered for the Green-Newmark Method and linear finite and boundary elements are adopted.

6.1 Infinite domain analysis

In the present application, the electromagnetic field surrounding an infinitely long wire, carrying a time-linear current, is studied (Soares and Vinagre, 2008; Soares, 2008). A sketch of the model and the adopted spatial discretizations are depicted in Fig.2: 2344 triangular finite elements and 80 boundary elements are employed in the analyses (the radius of the FEM-BEM interface is defined by $R = 1\,m$). For temporal discretization, the selected BEM time-step is given by $\Delta t_B = 2 \cdot 10^{-10} s$ and analyses considering $\Delta t_F = (1/8)\Delta t_B$ and $\Delta t_F = (1/16)\Delta t_B$ are carried out. The physical properties of the medium (air) are: $\mu = 1.2566 \cdot 10^{-6} H/m$ and $\varepsilon = 8.8544 \cdot 10^{-12} F/m$.

Fig.3 shows the modulus of the electric field intensity obtained at points A and B (see Fig.2) considering the two discussed FEM-BEM coupling algorithms. Analytical time histories (Machado, 2006) are also depicted in Fig.3, highlighting the good accuracy of the numerical results (one should notice that good accuracy is ob-

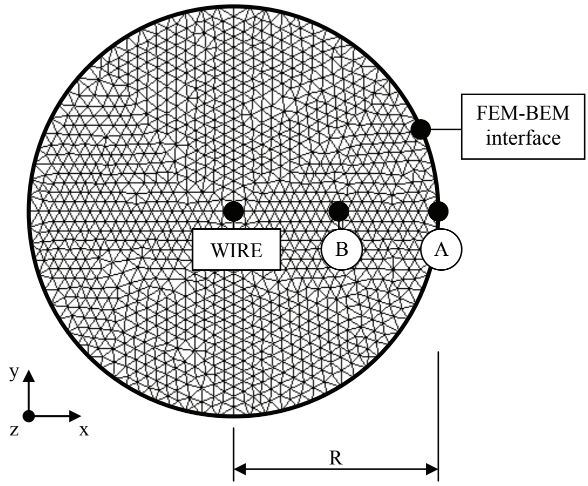

Figure 2: Sketch of the infinite domain model: circular FEM-BEM interface enclosing the FEM sub-domain and the centrally located wire.

served in spite of the quite different FEM/BEM time-steps considered, illustrating the robustness of the proposed methodologies).

In order to evaluate the efficiency of the proposed formulations, their CPU times were compared to those provided by an iterative FEM-BEM coupling approach, as described by Soares (2008) and implemented considering multi-level time-step discretizations. Taking into account the current application, the adoption of the explicit coupling procedures provides a CPU time reduction of, at least, 34% for $\Delta t_F = (1/8)\Delta t_B$ and 45% for $\Delta t_F = (1/16)\Delta t_B$. As one can observe, the proposed methodologies not only are robust, but also very efficacious.

6.2 Finite domain analysis

In this sub-section, two parallel lines of wires are considered and the electromagnetic field evolution within these lines is analysed. A sketch of the model and the adopted spatial discretizations are depicted in Fig.4: 40 square finite elements and 28 boundary elements are employed in the analyses (the geometry of the model is defined by $L = 1\,m$).

First, a homogeneous medium analysis is considered, and both materials 1 and 2 are air. The selected BEM time-step is given by $\Delta t_B = 2 \cdot 10^{-10}s$ and analyses considering $\Delta t_F = (1/4)\Delta t_B$ and $\Delta t_F = (1/8)\Delta t_B$ are carried out. Fig.5 shows the

(a)

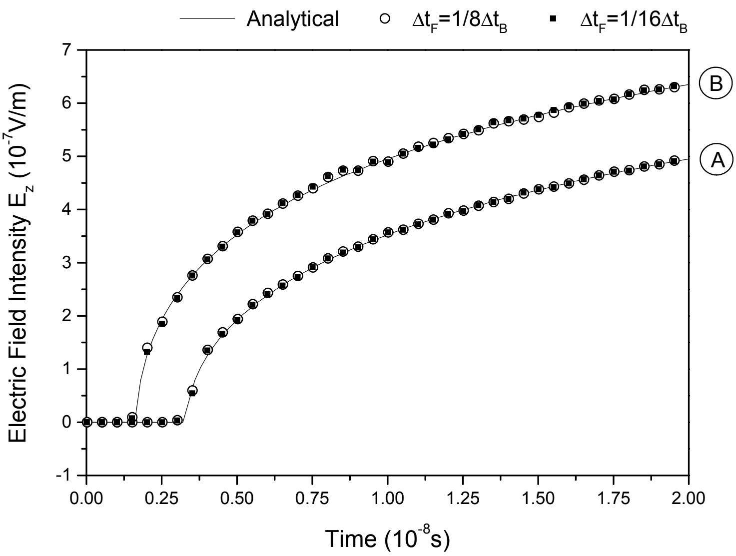

(b)

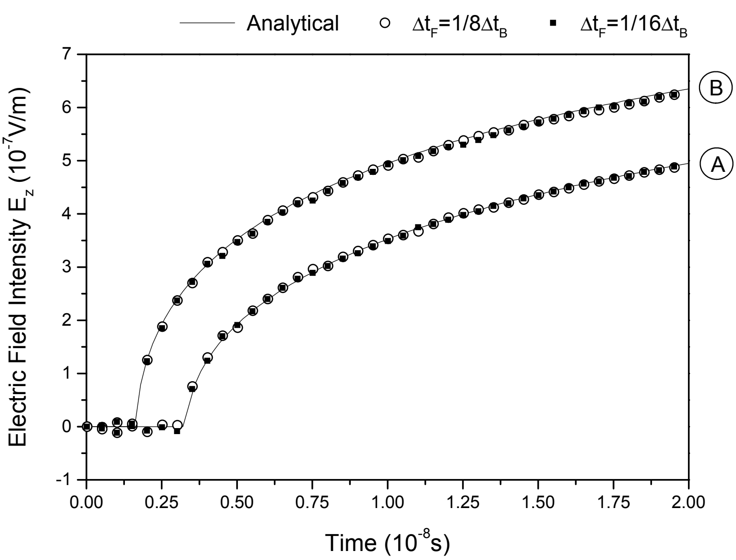

Figure 3: Time-history results for the electric field intensity at points A and B considering FEM-BEM coupled analyses and different temporal discretizations for each sub-domain: (a) algorithm 1; (b) algorithm 2.

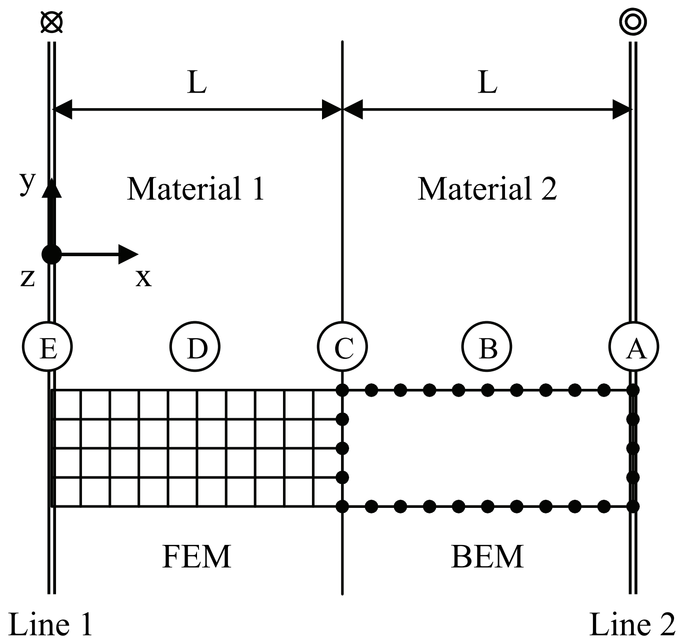

Figure 4: Sketch of the finite domain model: opposite lines of wires and sub-domains spatial discretizations.

electric field intensities obtained at points A, B, C, D and E (see Fig.4) considering the two FEM-BEM coupling algorithms. Analytical time histories (Miles, 1961) are, once again, also depicted in Fig.5, illustrating the good accuracy of the numerical results. It must be noticed that the application in focus is a very important benchmark since the analytical answer is known and it represents a rather complex numerical computation (in spite of its geometrical and load simplicity) once there are successive reflections occurring at the model extremities and these multiple reflections can emphasize some numerical aspects, such as instabilities and excessive numerical damping.

Taking into account time-domain BEM formulations, spurious oscillations may occur when bounded domains are analysed (in infinite domain analyses, these spurious oscillations are usually dissipated towards infinity). In order to avoid this kind of instabilities, the present work employs the multi-level time-step technique to be able to adopt optimal temporal discretizations for BEM sub-domains. Although, if additional procedures to smooth BEM results are necessary, the following refer-

(a)

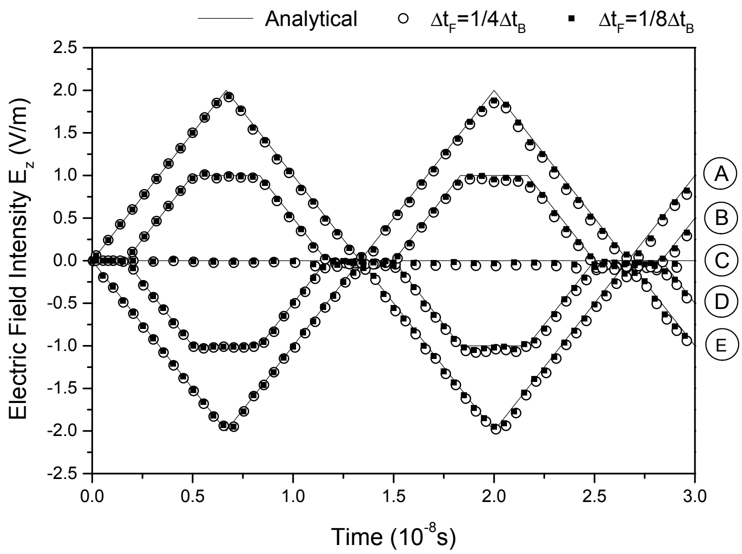

(b)

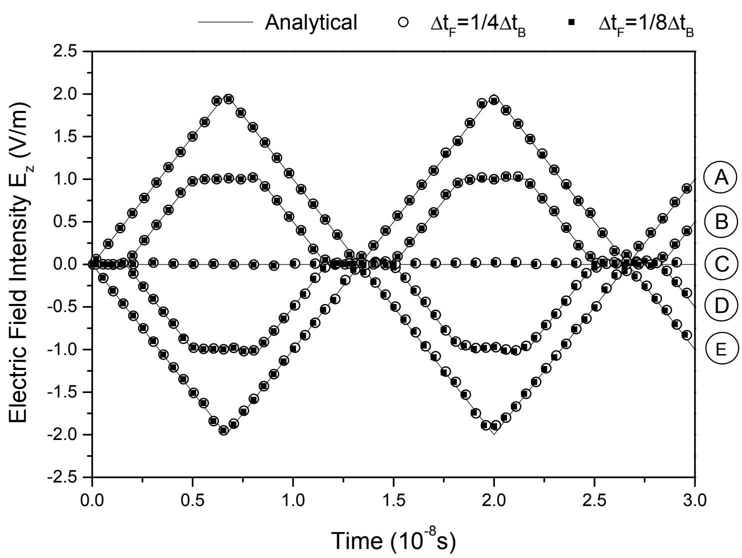

Figure 5: Time-history results for the electric field intensity at points A, B, C, D and E considering FEM-BEM coupled analyses and different temporal discretizations for each sub-domain (air-air model): (a) algorithm 1; (b) algorithm 2.

ences are indicated: Yu *et al.* (1998), Soares and Mansur (2007) etc..

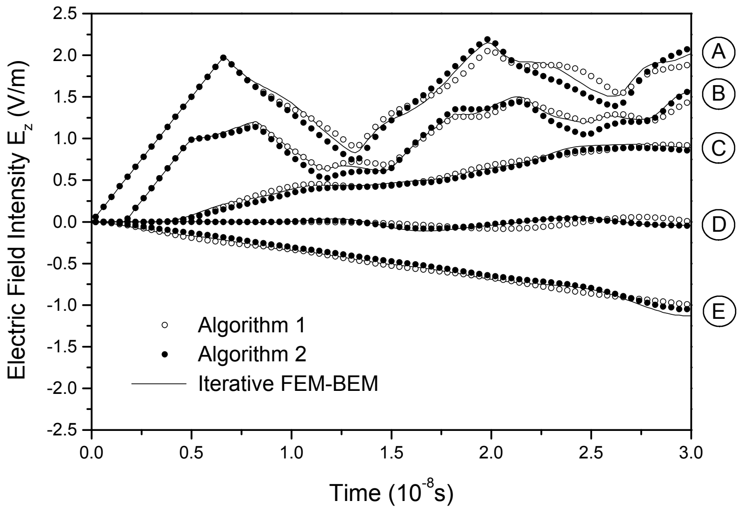

Figure 6: Time-history results for the electric field intensity at points A, B, C, D and E considering different FEM-BEM coupling procedures (air-water model).

A heterogeneous medium analysis is also carried out, considering material 1 as being water ($\varepsilon_R = 78$) and material 2 as air. In this case, the value of the wave propagation velocity in the FEM sub-domain is much lower, and the time discretization adopted can be given by: $\Delta t_F = \Delta t_B = 2 \cdot 10^{-10} s$. Time history results at points A, B, C, D and E are depicted in Fig.6, considering the two FEM-BEM coupling algorithms discussed here, as well as the iterative FEM-BEM coupling procedure (Soares, 2008). As can be seen, good agreement is observed. The discrepancy between the results depicted in Fig.6 is due to the adoption of lumped matrices **M** in equations (12) and in the last term of equation (16b) and consistent matrices in the iterative FEM-BEM coupling algorithm (one should observe that a poor spatial discretization is being considered). If a consistent matrix **M** is considered in equation (16b), the results related to the coupling algorithm 2 are visually the same as those related to the iterative FEM-BEM coupling, plotted in Fig.6.

7 Conclusions

In this work, two explicit time-domain FEM-BEM coupling algorithms are discussed. The formulations are very attractive since they allow each sub-domain of the global model to be independently and optimally treated (existing codes or computer programs can be easily employed in the coupled analyses once simple interface routines are implemented).

The FEM sub-domains are analysed considering time-marching procedures (namely the Central Difference Method, which is conditionally stable, and the Green-Newmark Method, which is unconditionally stable) which do not take into account the BEM field values at the present time-step and, as a consequence, the coupled system of equations can be properly uncoupled at the current time-step, rendering a very efficient methodology. Moreover, the coupling algorithms are discussed in conjunction with a multi-level time-step methodology, which allows considering better temporal discretizations within each sub-domain of the global model, improving the flexibility, accuracy and stability of the analyses.

At the end of the paper, numerical applications are considered, illustrating the good level of accuracy of the proposed formulations (one should observe that sub-domain time-step differences greater than fifteen times have been considered in the examples without any damage to the accuracy of the coupled analysis). In fact, the robustness and efficiency of the proposed algorithms are remarkable, improving the competitiveness of time-domain FEM-BEM coupling procedures to analyse complex electromagnetic models.

Acknowledgement: The financial support by CNPq (*Conselho Nacional de Desenvolvimento Científico e Tecnológico*) and FAPEMIG (*Fundação de Amparo à Pesquisa do Estado de Minas Gerais*) is greatly acknowledged.

References

Botha, M.M.; Jin, J.M. (2005): Adaptive Finite Element-Boundary Integral Analysis for Electromagnetic Fields in 3-D, *IEEE Transactions on Antennas and Propagation* vol. 53, pp. 1710-1720.

Eibert, T.F. (2007): Some Scattering Results Computed by Surface-Integral-Equation and Hybrid Finite-Element – Boundary-integral Techniques, Accelerated by the Multilevel Fast Multipole Method, *IEEE Antennas and Propagation Magazine* vol. 49, pp. 61-69.

Ha, T.; Seo, S.; Sheen, D. (2006): Parallel Iterative Procedures for a Computational Electromagnetic Modeling Based on a Nonconforming Mixed Finite Element Method, *CMES: Computer Modeling in Engineering & Sciences* vol. 14; pp. 57-76.

Jiao, D.; Ergin, A.A.; Shanker, B.; Michielssen, E.; Jin, J.M. (2002): A fast higher-order time-domain finite element – boundary integral method for 3-D electromagnetic scattering analysis, *IEEE Transactions on Antennas and Propagation* vol. 50, pp. 1192-1202.

Jiao, D.; Lu, M.; Michielssen, E.; Jin, J.M. (2001): A fast time-domain finite element – boundary integral method for electromagnetic analysis, *IEEE Transactions on Antennas and Propagation* vol. 49, pp. 1453-1461.

Liu, C.S. (2008): A New Mathematical Modeling of Maxwell Equations: Complex Linear Operator and Complex Field, *CMES: Computer Modeling in Engineering & Sciences* vol. 38; pp. 25-38.

Liu, J.; Jin, J.M. (2001): A Novel Hybridization of Higher Order Finite Element and Boundary Integral Methods for Electromagnetic Scattering and Radiation Problems, *IEEE Transactions on Antennas and Propagation* vol. 49, pp. 1794-1806.

Liu, J.; Jin, J.M. (2002): A Highly Effective Preconditioner for Solving the Finite Element–Boundary Integral Matrix Equation of 3-D Scattering, *IEEE Transactions on Antennas and Propagation* vol. 50, pp. 1212-1221.

Machado, K.D. (2006): *Teoria do Eletromagnetismo* – Vol.III, Ed. UEPG, São Paulo.

McCowen, A.; Radcliffe, A.J.; Towers, M.S. (2003): Time-domain modelling of scattering from arbitrary cylinders in two dimensions using a hybrid finite-element and integral equation method, *IEEE Transactions on Magnetics* vol. 39, pp. 1227-1229.

Miles, J.W. (1961): *Modern Mathematics for the Engineer* (E.F. Beckenbach, ed.), MacGraw-Hill, London.

Qiu, Z.J.; Xu, J.D.; Wei, G.; Hou, X.Y. (2007): An improved time domain finite element – boundary integral schem for electromagnetic scattering from 3-D objects, *Progress in Electromagnetism Research* vol. 75, pp. 119-135.

Soares Jr., D. (2007): A time-marching scheme based on implicit Green's functions for elastodynamic analysis with the domain boundary element method, *Computational Mechanics* vol. 40, pp. 827-835.

Soares Jr., D. (2008a): A time-domain FEM-BEM iterative coupling algorithm to numerically model the propagation of electromagnetic waves, *CMES: Computer Modeling in Engineering & Sciences* vol. 32, pp. 57-68.

Soares Jr., D. (2008b): A time-domain FEM approach based on implicit Green's functions for the dynamic analysis of porous media, *Computer Methods in Applied Mechanics and Engineering* vol.197, pp. 4645-4652.

Soares Jr., D.; Mansur, W.J. (2003): An efficient time/frequency domain algorithm for modal analysis of non-linear models discretized by the FEM, *Computer Methods in Applied Mechanics and Engineering* vol.192, pp. 3731-3745.

Soares Jr., D.; Mansur, W.J. (2005a): A time domain FEM approach based on implicit Green's functions for non-linear dynamic analysis, *International Journal for Numerical Methods in Engineering* vol. 62, pp. 664-681.

Soares Jr., D.; Mansur, W.J. (2005b): An efficient time-domain BEM/FEM coupling for acoustic-elastodynamic interaction problems, *CMES: Computer Modeling in Engineering & Sciences* vol. 8; pp. 153-164.

Soares Jr., D.; Mansur, W.J. (2007): An efficient stabilized boundary element formulation for 2D time-domain acoustics and elastodynamics, *Computational Mechanics* vol. 40, pp. 355-365.

Soares Jr., D.; Mansur, W.J.; von Estorff, O. (2007): An efficient time-domain FEM/BEM coupling approach based on FEM implicit Green's functions and truncation of BEM time convolution process, *Computer Methods in Applied Mechanics and Engineering* vol.196, pp. 1816-1826.

Soares Jr., D.; Vinagre, M.P. (2008): Numerical Computation of Electromagnetic Fields by the Time-Domain Boundary Element Method and the Complex Variable Method, *CMES: Computer Modeling in Engineering & Sciences* vol. 25, pp. 1-8.

Stupfel, B. (2001): A Hybrid Finite Element and Integral Equation Domain Decomposition Method for the Solution of the 3-D Scattering Problem, *Journal of Computational Physics* vol. 172, pp. 451–471.

Takei, A.; Yoshimura, S.; Kanayama, H. (2008): Large-Scale Parallel Finite Element Analyses of High Frequency Electromagnetic Field in Commuter Trains, *CMES: Computer Modeling in Engineering & Sciences* vol. 31; pp. 13-24.

Tzoulis, A.; Eibert, T.F. (2005): A Hybrid FEBI-MLFMM-UTD Method for Numerical Solutions of Electromagnetic Problems Including Arbitrarily Shaped and Electrically Large Objects, *IEEE Transactions on Antennas and Propagation* vol. 53, pp. 3358-3366.

Yılmaz, A.E.; Lou, Z.; Michielssen, E.; Jin, J.M. (2007): A Single-Boundary Implicit and FFT-Accelerated Time-Domain Finite Element-Boundary Integral Solver, *IEEE Transactions on Antennas and Propagation* vol. 55, pp. 1382-1397.

Young, D.L.; Ruan, J.W. (2005): Method of Fundamental Solutions for Scattering Problems of Electromagnetic Waves, *CMES: Computer Modeling in Engineering & Sciences* vol. 7; pp. 223-232.

Yu, G.; Mansur, W.J.; Carrer, J.A.M.; Lei, G. (1998): A linear θ method applied to 2D time domain BEM analysis, *Communications in Numerical Methods in Engineering* vol.14, pp. 1171-1179.